small methods
www.small-methods.com

On Surface Synthesis of Sp-Hybridized Carbon Allotropes

*Yuan Guo, Wenzhi Xiang, Luye Sun, and Wei Xu**

Carbon allotropes have been extensively studied due to their unique structures and properties. Carbon exists in three hybridization states, among which sp-hybridized carbon allotropes are particularly challenging to synthesize due to their high reactivity. On-surface synthesis methods have emerged as a promising approach for the generation and characterization of such carbon allotropes. In this review, recent experimental efforts are summarized in the synthesis of sp-hybridized carbon allotropes, including linear carbon chains and cyclo[*n*]carbons on surfaces.

1. Introduction

Carbon is one of the most abundant elements in the universe, occurring in a multitude of forms in both living organisms and inorganic matter.[1] The diverse structural forms of carbon allotropes are related to the various hybridization states of carbon when forming bonds, including sp, sp^2, sp^3 configurations.[2] Carbon's versatile bonding capabilities allow it to form a wide range of structural configurations with unique properties.[3–5] Naturally formed carbon allotropes include graphite and diamond. Sp^2-hybridized graphite is known for its high thermodynamic stability and a high natural abundance, while for the sp^3-hybridized diamond, its formation requires the presence of elevated temperatures and pressures.[6–8] Both forms exhibit distinctive physical and chemical properties, including the high conductivity and self-lubricating properties observed in graphite and the high hardness exhibited by diamond.[9–11] The development of an artificial synthesis method has opened up new avenues for the study of novel carbon allotropes. In 1985, Kroto and co-workers made a fortuitous discovery when they irradiated graphite with high-power laser pulses, leading to the formation of the C_{60} molecule.[12–14] The C_{60} molecule is composed of 12 five-membered rings and 20 six-membered rings of sp^2-hybridized carbon atoms, forming a hollow, highly symmetrical globular structure.[12] This unique configuration endows the molecule with remarkable stability, superior electrical conductivity to Cu, and high strength.[15] A tubular structure, carbon nanotubes consisting of sp^2-hybridized atoms, have been synthesized by Iijima et al. in 1991,[16] performing high mechanical strength, good flexibility and high electrical conductivity.[16,17] These attributes render them optimal additives for polymer composites.[18] In 2004, Geim and Novoselov isolated a single layer of carbon atomic structure, i.e., graphene, from graphite through the innovative application of mechanical exfoliation.[19] Graphene consists of sp^2-hybridized atoms, and is celebrated for its remarkable physical properties, including a Young's modulus of 1 TPa and a tensile strength of 130 GPa, which contribute to its remarkable mechanical robustness.[20,21] Additionally, it exhibits an electrical conductivity of 10^6 S m^{-1} and a carrier mobility higher than 10^4 cm^2/Vs, which are also noteworthy. Graphene has excellent properties: high electrical conductivity (10^6 S m^{-1}), carrier mobility, 97.7% optical transparency, good thermal management (theoretical 5300 W mK^{-1}, measured 5.3 ± 0.48 × 10^3 W mK^{-1}), and outstanding stability under extreme conditions (melting point 4125–5000 K), suitable for various applications.[19–25] A novel carbon allotrope, Gradia, is composed of coherently bonded graphite and diamond nanodomains.[26,27] Synthesized by controlling the direct graphite-to-diamond phase transformation, Gradia combines the hardness of diamond with the toughness of graphite, while also exhibiting tunable electrical properties.[28,29] This unique combination of characteristics makes it a promising material for applications in mechanics, electronics, and energy storage.[30] The discovery of these special carbon materials has further stimulated the scientific interest in the field of other carbon forms, especially sp-hybridized allotropes. In the 1960s, early traces were found within a German crater called Chaoite,[31] i.e., sp-hybridized linear carbon. They have also been detected in space, including comets, sunspots, stars and interstellar clouds.[32–34] Theoretical works predicated that carbon chains possess very high tensile strength and electrical conductivity at room temperature, showing great potentials for various mechanical and electronic applications.[35] There has long been a controversy regarding the most stable structures, whether linear carbon or its cyclic form, i.e., cyclo[*n*]carbon.[5,32,36–40] Cyclo[*n*]carbon also are predicated as precursors in the synthesis of fullerenes and other similar substances.[41] In flames, they contribute to the complex chemical reactions taking place, and they act as crucial intermediates in the plasmas harnessed to fabricate thin films of diamond.[37,42] However, due to the high reactivity associated with sp-hybridization, the synthesis of these molecules in solution is extremely challenging, leaving their structures and properties largely unexplored.[43,44] For sp-hybridized carbon chains, there is a tendency to react and crosslink to form sp^2 and sp^3 carbon systems.[43,44] Carbon polyynes

Y. Guo, W. Xiang, L. Sun, W. Xu
Interdisciplinary Materials Research Center
School of Materials Science and Engineering
Tongji University
Shanghai 201804, P. R. China
E-mail: xuwei@tongji.edu.cn

The ORCID identification number(s) for the author(s) of this article can be found under https://doi.org/10.1002/smtd.202500119

DOI: 10.1002/smtd.202500119

without end groups typically have radicals, making them highly reactive.

On-surface synthesis method has emerged as a powerful technique for the creation of novel carbon allotropes.[45–49] This method through ultra-high vacuum (UHV) systems allows for precise control over the growth, assembly and reactions of carbon structures on a substrate, enabling the production of materials that are difficult to obtain by traditional methods.[50,51] Scanning tunneling microscopy (STM) and atomic force microscopy (AFM) are powerful techniques in performing structural and electronic characterization in situ.[52,53] Solid substrates, especially metal substrates usually provide good sites as supporting templates and more importantly, as catalysts to induce surface reactions. Metal-induced surface reactions are regulated by thermodynamic and kinetic processes.[54] This approach, exemplified by the work of Grill and colleagues in 2007, has demonstrated substantial outcomes, notably the formation of covalent couplings of tetraphenyl-porphyrins.[55,56] In 2021, Fan et al. achieved to synthesize a biphenylene network, a nonbenzenoid carbon allotrope through an on-surface interpolymer dehydrofluorination reaction.[57]

Another way to trigger reactions is tip-induced manipulation, helping to synthesize lots of highly reactive species on the surface.[58] Tip-induced manipulation represents a precision synthesis technique at the single-atom level, allowing for the precise manipulation of molecules adsorbed on a surface through the operation of a STM tip, leading to molecular dissociation, diffusion, bonds formation and rearrangement, as well as alteration of the conformation or charge state.[59] For example, Hla and colleagues employed STM tips to facilitate the Ullmann reaction in 2000, demonstrating the control of chemical reactions at room temperature.[60] Recently, a series cyclo[*n*]carbons have been generated on the surface via tip-induced manipulation.[61–65]

This review is organized as follows: First part focuses on the synthesis and characterization of the metalated carbyne and linear carbon chains via metal-induced surface reactions. Second part focuses on the synthesis and characterization of cyclo[*n*]carbons via tip manipulation. Last part extends related techniques which can help further research these.

2. Linear Carbon Chains

Linear carbon chains (LCCs) refer to atomic wires consisting of the sp-hybridized carbon atoms.[66] Infinite LCC, namely carbyne, has been predicated owing many remarking properties.[67,68] Carbyne is an exceptionally strong and stiff material with a specific strength of up to 7.5×10^7 N m kg^{-1}, requiring ≈10 nN to break a single atomic chain. It can be transitioned into a magnetic semiconductor state through mechanical twisting and exhibits a remarkable Young's modulus of 32.7 TPa.[35] Carbyne also shows a significant coupling between strain and bandgap, increasing from 2.6 to 4.7 eV under a 10% strain, and demonstrates chemical stability against self-aggregation with an activation barrier of 0.6 eV for carbyne-carbyne cross-linking. These properties make carbyne a promising candidate for nanoscale electrical cable applications and highlight its potential in the field of materials science.[35]

LCCs can be classified into two distinct resonance structures: a cumulenic structure comprising continuous carbon-carbon double bonds and a polyynic structure featuring alternating single and triple carbon-carbon bonds.[69,70] It is sometimes the case that for infinite LCCs, polyyne is designated as α-carbyne, whereas cumulene is referred to as β-carbyne.[71] Peierls theory predicated that for infinite LCC, polyynic structure possesses a bandgap, exhibiting semiconductor behavior, while cumulenic structure displays metallic properties.[72] For finite LCCs, their detailed structures may be influenced by other terminal groups.[73] Hydrogen-capped polyynes present an alternated structure due to single bond from –CH terminal group. While vinylidene group (i.e., $=CH_2$) presents with a double bond at the terminal, inducing the formation of cumulenic structures.

2.1. Synthesis of Metallated Carbyne

Metalated carbyne is a distinctive structure that incorporates both metal and carbon atoms. With a pattern of alternating single and double bonds, metalated carbyne could manifest as semiconductors. Experimentally, metalation of carbyne with regularly distributed metal atoms is very challenging.[74] Here, we introduce recent progresses on the preparation of metalated carbyne and their characterizations.

An efficient method for the synthesis of metalated carbyne by Sun et al., was shown in **Figure 1a**$_{I}$.[75] Using the C_2H_2 molecules as precursors, metalated copper carbyne (C_2Cu polymer) was synthesized by molecular dehydrogenations and polymerizations. Taking advantage of the high chemical activity of Cu(110) and the 1D template effect, the chain length was extended to the submicron scale. The bright protrusions in STM image (Figure 1a$_{II}$) correspond to the copper atoms within the chains. Non-contact AFM (nc-AFM) images reveal characteristic bright features between copper atoms, representing carbon-carbon triple bonds (Figure 1a$_{III,IV}$). The periodicity displayed in the image, ≈5.2 ± 0.2 Å, aligned well with the model optimized by density functional theory (DFT) calculations.

Using C_4Br_4 molecules as the precursors, Xin and colleagues successfully synthesized the metalated Au carbyne (C_4Au polymer) on Au(111) surface (Figure 1b$_{I}$).[76] The bright protrusions in the STM images also represent the positions of Au atoms (Figure 1b). An interesting observation (Figure 1c) is that using tip manipulation, a transformation from cumulene (C_4Br_4) to polyyne (C_4Br_2) is achieved at liquid helium temperature. The electronic state information of this C_4Au polymer was also detected on Au, with the valence band maximum observed at 1.5 V and the conduction band minimum at −0.5 V, corresponding to a calculated intrinsic electronic structure with a density of states (DOS) gap of 2.6 eV (Figure 1e). A ring precursor, C_6Br_6, also enables the formation of metalated carbyne (C_6Ag polymer) through dehalogenation and ring-opening reactions.[77] Upon deposition on the Ag(111) surface at 300 K, densely packed striated structures are observed. As illustrated in the accompanying Figure 1c, Ag is visualized as protrusions in STM (Figure 1c$_{IV}$) and as depressions in AFM (Figure 1c$_{V}$). These structures on the

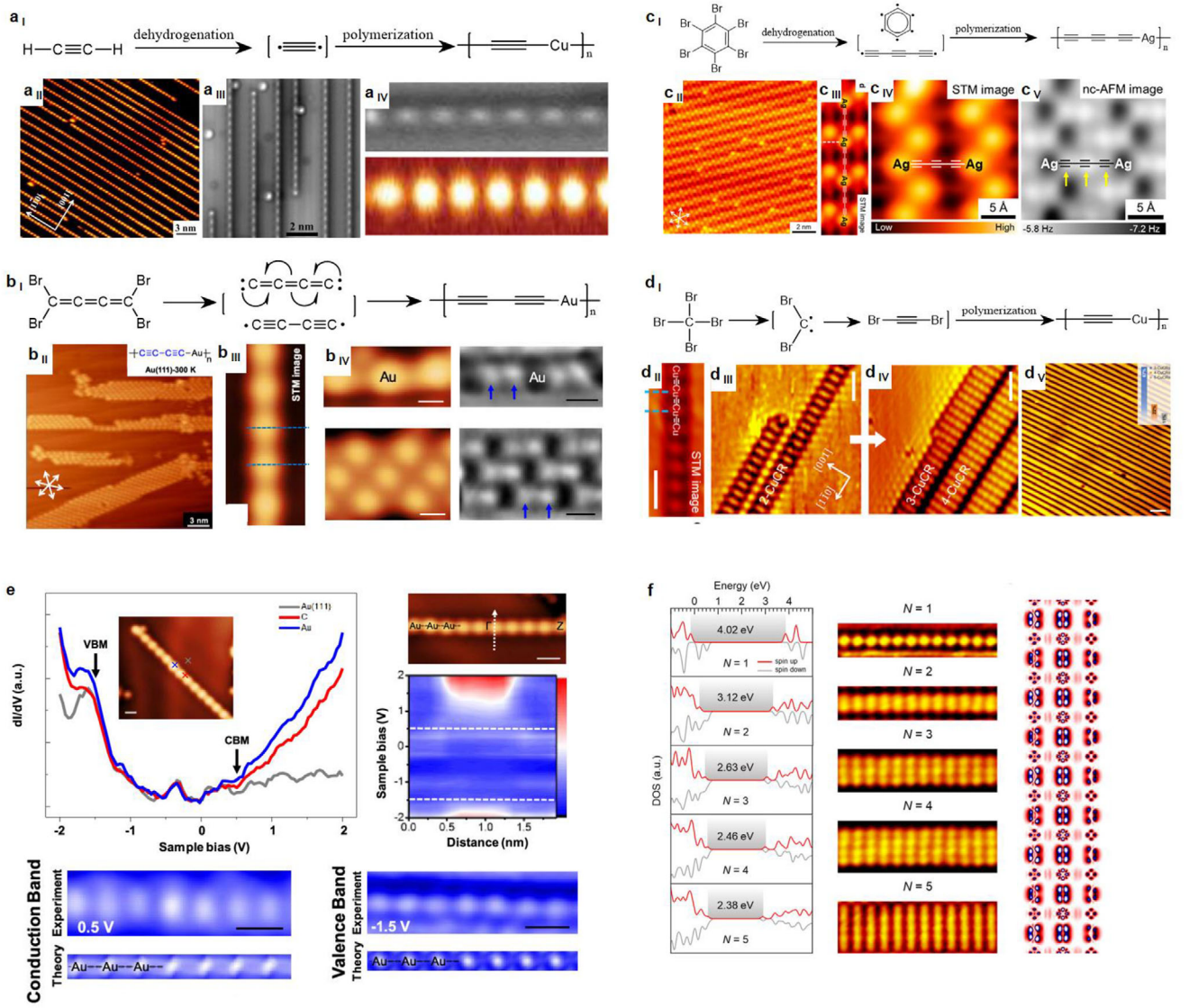

Figure 1. On-surface synthesis of metalated carbyne. a_I to a_{IV}) The dehydrogenative coupling of ethyne precursors to form Cu carbyne on Cu(110). Reproduced with permission.[75] Copyright 2016, American Chemical Society. b_I to b_{IV}) Formation of C_4Au by polymerization from a cumulene moiety to an organometallic polyyne on the Au(111) surface. Reproduced with permission.[76] Copyright 2020, American Chemical Society. c_I to c_V) Formation of organometallic polyyne on the Ag(111) surface by dehydrogenations and polymerization of C_6Br_6. Reproduced with permission.[77] Copyright 2022, American Chemical Society. d_I to d_V) Synthesis of CuCRs via α- and β-elimination reactions on Cu(110). Reproduced with permission.[78] Copyright 2023, American Chemical Society. e) Electronic characterization of Au carbyne. f) Electronic properties of CuCRs with different widths.

Ag(111) surface also exhibit semiconductor properties, with an energy bandgap of 1.3 eV.

Upon depositing fully brominated molecules (CBr_4 and C_2Br_6) onto metallic substrates at 300 K, elongated chains oriented along the [1$\bar{1}$0] direction were successfully synthesized on both Cu(110) and Ag(110) surfaces.[78] As depicted in Figure 1d, upon progressive annealing of the sample, the chains assemble together and evolve into ribbon-like structures. Through wave function analysis of interchain interactions and the corresponding DOS, it is revealed that the interactions between the chains are primarily dominated by copper. As the width of the merged chains increases from 1 to 5, the corresponding bandgap decreases from 4.02 to 2.38 eV (Figure 1f).

The substrate significantly impacts the desorption temperature, reactivity, and electronic properties of carbon chains. On Cu(110), the carbon chains desorb at ≈550 K,[75] while they desorb at ≈ 450 K on Au(111),[76] ≈ 380 K on Ag(111).[77] The substrate also greatly influences reactivity; for instance, acetylene molecules react on Cu(110) within the temperature range of 180 K to 600 K, but they do not react on Ag(111) and Au(111) within this range.[75] Furthermore, the substrate affects the electronic properties of carbon chains, for example, the bandgap of metal-carbon chains synthesized on different metal substrates is different. The bandgap of Ag carbyne ribbons on Ag(111) is larger than that of Cu carbyne ribbons (CuCRs) on Cu(110).[78]The extension to other

metals (e.g., iron atoms) presents challenges but warrants further exploration.[79,80]

2.2. Synthesis of Linear Carbon Chains

Building upon metalated carbyne, Gao and colleagues have recently employed this method to further synthesize and characterize LCCs.[81] By depositing 1,1,2,3,4,4-hexabromobutadiene (C_4Br_6) molecules on Au(111) at 300 K and undergoing dehalogenation reactions and polymerization, metalated gold carbyne was formed on surface. After annealing at 380 K for 60 min, the formation of LCCs in the metalated gold carbyne was observed. It was found that metalated gold carbyne interacts more strongly with the metal substrate, resulting in a lower adsorption height. Extending the heating time at 380 K to 1 h led to the elongation of the LCCs (**Figure** 2a$_I$). The longest LCC observed consisted of ≈60 alkyne units (120 carbon atoms), as deduced from its length of ≈ 15 nm. Experimentally observed Br islands can partially decouple the LCCs by the intercalation. As shown in Figure 2a, two resonance peaks are observed at −2.8 and 0.87 V, attributed to the highest occupied molecular orbital (HOMO) and the lowest unoccupied molecular (LUMO), respectively, yielding a gap of ≈3.67 eV. The constant height dI/dV mapping at 0.87 V reveals characteristic nodes between each triple bond that correspond to the LUMO, which is consistent with DFT calculations.

Tip-induced manipulation has also employed to synthesize LCCs with end groups. In 2018, Pavliček et al. were inspired by the Fritsch–Buttenberg–Wiechell (FBW) rearrangement and achieved the reductive rearrangement of a 1,1-dibromoolefin to an alkyne (Figure 2b).[82] Initially, the tip is positioned above or in close proximity to the molecule. By applying consecutive voltage pulses greater than 1.4 V to remove bromine atoms, a diradical is obtained, existing in an isomer form with bromine atoms pointing toward the center of the molecule. Further debromination yields the final product, hexayene. For the LUMO of a neutral molecule, a sufficiently large positive or negative sample bias can attach electrons to the molecule or detach electrons from it (Figure 2c). The corresponding voltage for tunneling through negative ion resonance (NIR)/positive ion resonance (PIR) reflects the density of LUMO/HOMO. Notably, NIR corresponds to the characteristic nodes between each triple bond in the LUMO. As the chain lengthens, a continuous decrease in LUMO energy and a reduction in the bandgap are observed.

Recently, Gao et al. used tip manipulation to synthesize C_{14} chains.[81] They chose a fully halogenated molecule, $C_{10}Cl_{14}$, as the precursor. Via tip-induced dehalogenation and ring-opening reactions, a linear chain (C_{14}) was generated on the NaCl surface, and further characterized as a polyynic structure via nc-AFM (Figure 2f). Benefiting from the decoupling effect of the NaCl films, they successfully obtained the transport gap of C_{14} ≈ 5.8 eV.[81]

3. Cyclo[*n*]Carbons

Cyclo[*n*]carbons are molecular carbon allotropes consisting of rings of sp-hybridized carbon atoms.[83,84] Compared to linear carbon chains, cyclo[*n*]carbons are structures where the chain is connected end-to-end to form a cyclic arrangement.[85] Despite the apparent simplicity of cyclocarbon molecules, theoretical predictions about their structures and stabilities have often been controversial.[37,86–89] Their precise structures are often under debate on the cumulene or polyyne, depending on the different of theory.[40,87] In addition, their relative stabilities compared to linear one are also unknown. Roald Hoffmann predicated that for carbon clusters (C_n), a ring form could be more stable than its linear chain counterparts when $n \geq 10$.[90,91] When synthesizing cyclocarbons, precise control of experimental conditions is crucial. The process typically occurs at liquid helium temperature under UHV to stabilize reactive intermediates. First, specific halogenated precursors are thermally sublimated onto cold substrates. A common substrate is a thin NaCl film on an Au(111) surface or Cu(111) surface, which provides a stable and inert platform. Then, tip manipulation and characterization rely on advanced microscopy techniques: STM tip can remove the protected groups, breaking chemical bonds and induced ring-opening reactions, while AFM, especially with CO-functionalized tips, offers high-resolution imaging of carbon skeletons, halogen atoms, and triple bonds. These techniques collectively enable the detailed study of cyclocarbons and support their potential applications in nanotechnology and materials science. Recently, on-surface synthesis methods have been employed to generate a series of cyclocarbons, including C_{10}, C_{12}, C_{13}, C_{14}, C_{16}, C_{18}, C_{20}, and C_{26}, and characterized using bond-resolved AFM, providing insights into their structures and stabilities.

3.1. On-Surface Synthesis and Structural Characterization of Cyclo[*n*]Carbons

Recently, tip manipulation has been demonstrated to be the powerful way to generate highly reactive molecules, like cyclocarbons. Employing this approach, in 2019, Kaiser et al. used the $C_{24}O_6$ molecule as the precursor, to generate cyclo[18]carbon, C_{18}.[61] This molecule was first synthesized in 1990 by Diederich et al, and is inherently unstable.[92] After depositing the precursor on a thin insulating NaCl partially covered on Cu(111) surface, AFM images revealed an intact molecule exhibiting a triangular configuration. The dark features at the vertices correspond to the carbonyl groups (**Figure** 3a). The characteristic bright features on each side of the molecule represent the triple bonds. Via applying volage pulses, two, four, or six CO groups could be selectively removed from the molecule. The C_{18} product in Figure 3a shows a ring with nine characteristic bright features, indicating a polyynic structure rather than cumulenic one. In 2020, they use another similar precursor $C_{18}Br_6$ to generate C_{18}, and achieved a higher yield ≈ 64%, significantly higher than the 13% yield achieved with $C_{24}O_6$.[93] The literature also demonstrate that AFM (Figure 3b$_{III}$) cannot distinguish the polyynic C_{18} with or without bond angle alternation. These results stimulate much theoretical works on the cyclocarbons.[94–101]

According to the Hückel rule ($n = 4k + 2$, k is an integer), C_{18} is aromatic.[102] While for anti-aromatic cyclocarbons, generation of them could be more challenging.[91,103] In 2023, Gao et al. used another precursor, $C_{16}(CO)_4Br_2$, to synthesize the cyclo[16]carbon (Figure 3c).[64] Via tip-induced debromination and decarboxylation, C_{16} was generated on the surface, and

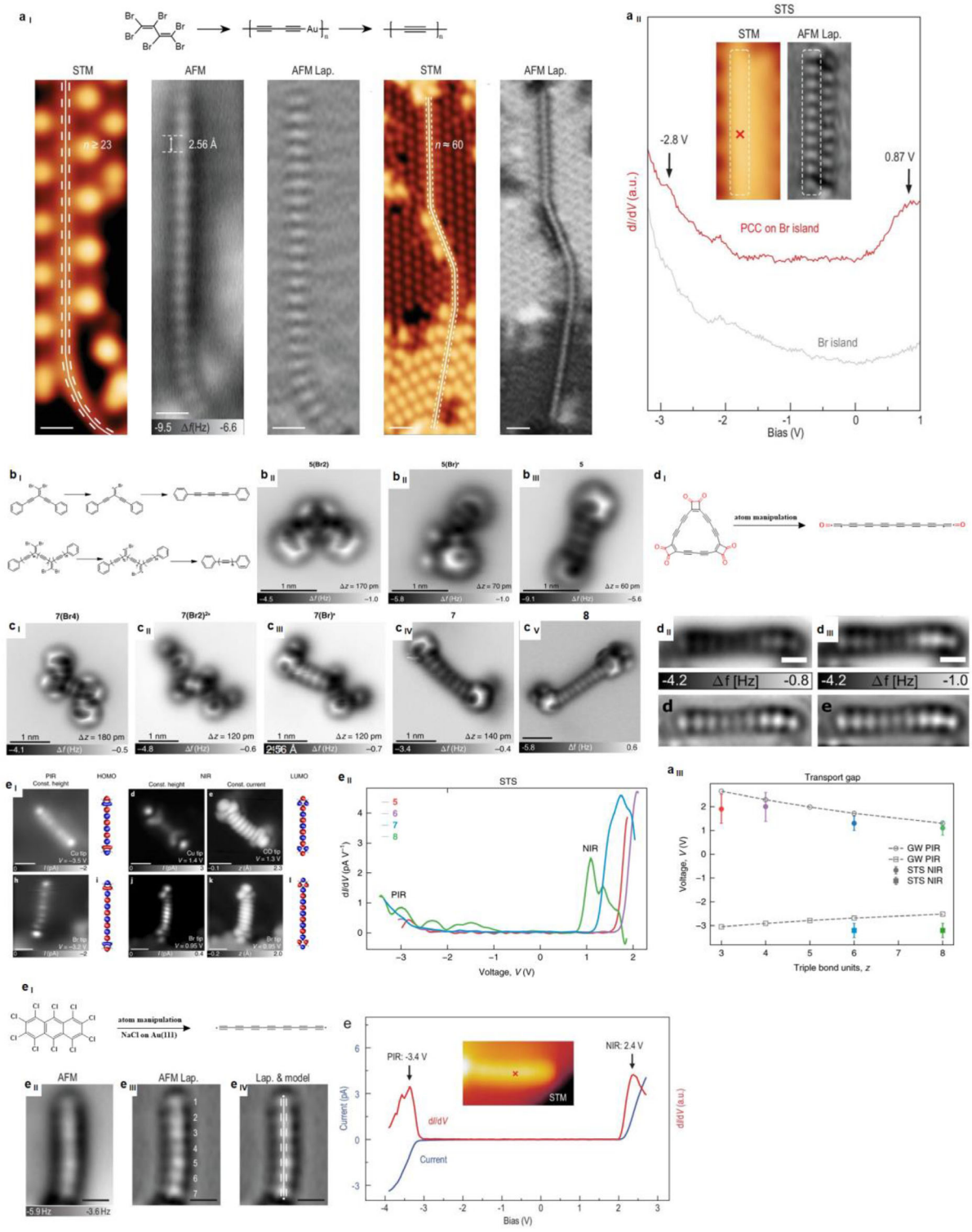

Figure 2. On-surface synthesis of polyynic carbon chain a $_{I}$) Formation of LCCs with the longest one observed consisting of ~60 alkyne units. a $_{II}$) The d*I*/d*V* spectrum of the LCC segment on Br island. Reproduced with permission.[81] Copyright 2024, The Author(s) 2024. Published by Oxford University Press on behalf of China Science Publishing & Media Ltd. b) On-surface synthesis of triyne and octayne on bilayer NaCl on Cu (111). Reproduced with permission.[82] Copyright 2018, Springer Nature. c) Synthesis of $C_{18}O_2$ chain by atom manipulation with precursor $C_{24}O_6$. c $_{II}$-c $_{V}$) Nc-AFM image and corresponding Laplace-filtered nc-AFM images. Reproduced with permission.[61] Copyright 2019, AAAS. d) STM images of the PIR and NIR with different tip terminations, STS of polyynes 5–8 and transport gap as a function of triple bond units. e) On-surface synthesis and characterization of C_{14} polyyne. e $_{II}$-e $_{IV}$) AFM image, Laplace-filtered nc-AFM images of a polyyne with 7 alkyne units. e$_{V}$) The d*I*/d*V* spectrum of C_{14} polyyne on NaCl/Au(111) acquired at different position.

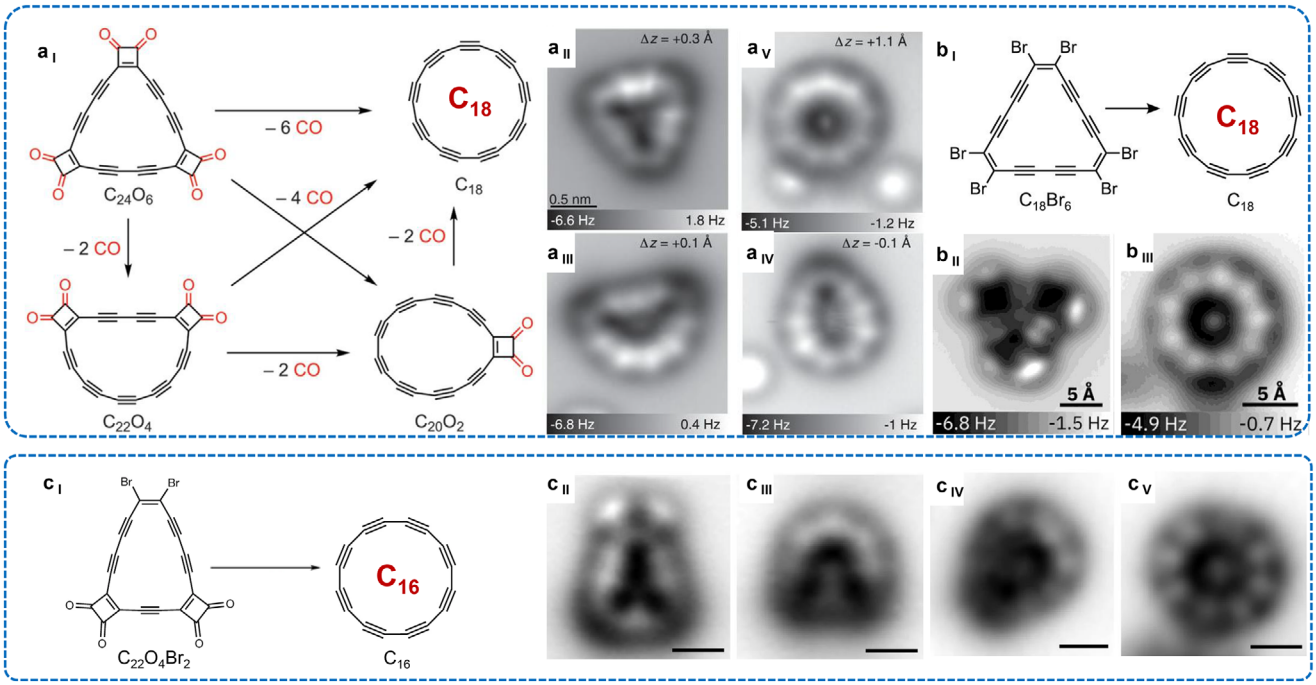

Figure 3. On-surface synthesis of cyclo[18]carbon and cyclo[16]carbon. a $_{I}$) Reaction scheme for the on-surface formation of C_{18}. a $_{II}$-a $_{V}$) AFM images of precursor $C_{24}O_6$, intermediate $C_{22}O_4$, intermediate $C_{20}O_2$ and final product C_{18}, respectively. Reproduced with permission.[61] Copyright 2019, American Association for the Advancement of Science. b $_{I}$) Synthesis of cyclo[18]carbon via $C_{18}Br_6$. b $_{II}$-b $_{III}$) AFM images of $C_{18}Br_6$ acyclo[18]carbon. Reproduced with permission.[93] Copyright 2020, American Chemical Society. c $_{I}$) Reaction scheme of synthesis of cyclo[16]carbon. c $_{II}$-c $_{V}$) AFM images of precursor $C_{20}O_4Br_2$, intermediate $C_{20}O_4$, intermediate $C_{18}O_2$ and final product C_{16}, respectively. Reproduced with permission.[64] Copyright 2023, The Author(s).

characterized also as a polyynic structure (Figure 3c$_{v}$), same to the case of C_{18}. Besides C_{16}, literature also tried the synthesis of other anti-aromatic cyclocarbons, like C_{20} and C_{24}, using $C_{28}O_8$ and $C_{32}O_8$. However, due to the very high reactivity, after the sublimation treatment, precursor molecules were found to be broken.

In 2023, Sun et al employed a new kind of precursors to synthesize cyclocarbons, that is, fully halogenated molecules.[63] Early literature has demonstrated the feasibility of tip-induced retro-Bergman ring-opening on the surface.[104] They have demonstrated that through tip-induced dehalogenation and retro-Bergman ring-opening reactions, a series of cyclocarbons can be generated on the surface.[62,63,65] They first aim to synthesize a smaller cyclocarbon, C_{10}. Modern theoretical works have predicted that C_{10} adopts a cumulenic structure, rather than polyynic one. Using a fully halogenated naphthalene molecule, $C_{10}Cl_8$, and via tip-induced dehalogenation and accompanied retro-Bergman reactions, the final product C_{10} can be generated on the surface. The AFM image in **Figure** 4a of C_{10} exhibits a uniform feature, which is consistent with the structure of cumulene, different from C_{18} and C_{16}.

Cyclo[14]carbon, another aromatic molecule, has been theoretically predicated as an intermediate between the cumulenic C_{10} and the polyynic C_{18}. Employing the same strategy used in C_{10}, a fully halogenated anthracene, $C_{14}Cl_{10}$, was synthesized and evaporated on the surface. Via the tip-induced complete dehalogenation and two steps of retro-Bergman ring-opening reactions, C_{14} was synthesized on the surface (Figure 4b), and characterized as a cumulenic structure, similar to C_{10}, as its bond length alternation (BLA) of 0.05 Å could not be distinguished through AFM imaging. AFM simulations of C_{14} molecules with varying BLAs show that when BLA ≥ 0.09 Å, the characteristic bright features of triple bonds could be more clearly distinguished.

Retro-Bergman ring-opening reaction was extended to synthesize anti-aromatic cyclocarbons. In 2024, Sun et al. designed a fully halogenated precursor containing four-numbered ring, $C_{12}Br_4I_4$, aiming to synthesize the C_{12}.[65] Via the tip-induced complete dehalogenation and two steps of retro-Bergman ring-opening reactions, C_{12} was synthesized on the surface, and characterized as a polyynic structure, similar to C_{16} (Figure 4d). Notably, it was found that the thickness of NaCl can be used to control the yield of C_{12}. With the thickness of NaCl layers increased, the yield of C_{12} decreased, as the disturbance of intermediates during imaging on the NaCl surfaces. Additionally, through on-surface transformation from hexagonal-tetragonal (6-4) carbon ring structures to pentagonal (5-5) carbon structures, followed by dehalogenation and more complex ring-opening reactions, such as retro-Bergman and Sondheimer-Wong diyne reactions, cyclocarbon C_{20} was successfully synthesized, and characterized as a polyynic structure (Figure 4e), same to the case of C_{12} and C_{16}.

Most recently, this strategy also was used to synthesize the odd-numbered cyclocarbon, C_{13}.[62] Voltage pulses were applied to decachlorofluorene ($C_{13}Cl_{10}$) to remove the Cl atoms, followed by retro-Bergman ring-opening reactions, resulting in the formation of C_{13} (Figure 4e) Various structures of C_{13} were observed, including a round shape and a more distorted kinked geometry

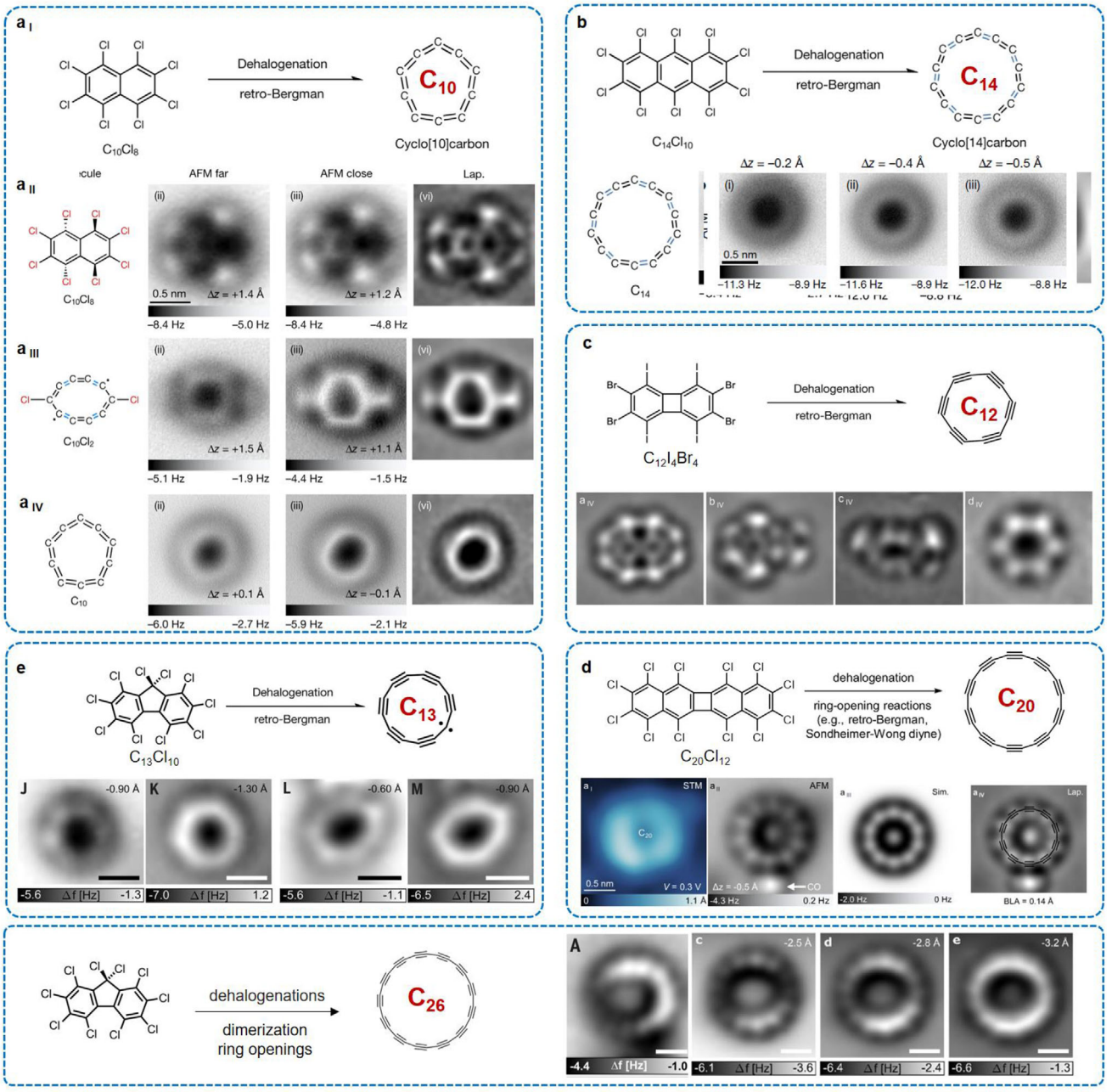

Figure 4. On-surface synthesis of cyclo[10]carbon, cyclo[14]carbon, cyclo[12]carbon, cyclo[20]carbon, cyclo[13]carbon and cyclo[26]carbon. a) Synthesis of cyclo[10]carbon via dehalogenation and retro-Bergman reaction of $C_{10}Cl_8$. a $_{II}$-a $_{IV}$) Chemical structure, AFM images (far and close), Laplace-filtered AFM images of precursor $C_{10}Cl_8$, intermediate $C_{10}Cl_2$ and final product C_{10}. Reproduced with permission.[63] Copyright 2023, The Author(s), under exclusive licence to Springer Nature Limited. b) The top half of the figure is schematic illustration of the synthetic route to C_{14}. Bottom half of the figure is AFM image at different tip heights and corresponding Laplace-filtered AFM images. c) The upper portion of the figure corresponds to the scheme of synthesis of C_{12} from $C_{12}Br_4I_4$. Lower portion shows the Laplace-filtered AFM images of precursor $C_{12}Br_4I_4$, intermediate $C_{12}Br_4I_2$, intermediate $C_{12}Br_3$ and final product C_{12}, respectively. Reproduced with permission[65] Copyright 2024, The Author(s). d) The upper section of the figure is schematic illustration of formation of C_{20} by dehalogenation, ring-open reaction (retro-Bergman and Sondheimer-Wong diyne) of $C_{20}Cl_{12}$. The lower section is analogous to STM image, AFM image, simulation and Laplace-filtered AFM image of C_{20}. e) Scheme for the synthesis of C_{13} from $C_{13}Cl_{10}$ and AFM image of different geometry. Reproduced with permission.[62] Copyright 2024, The Authors. f) Synthesis of C_{26} through dehalogenation, ring openings and dimerization reaction of $C_{13}Cl_{10}$.

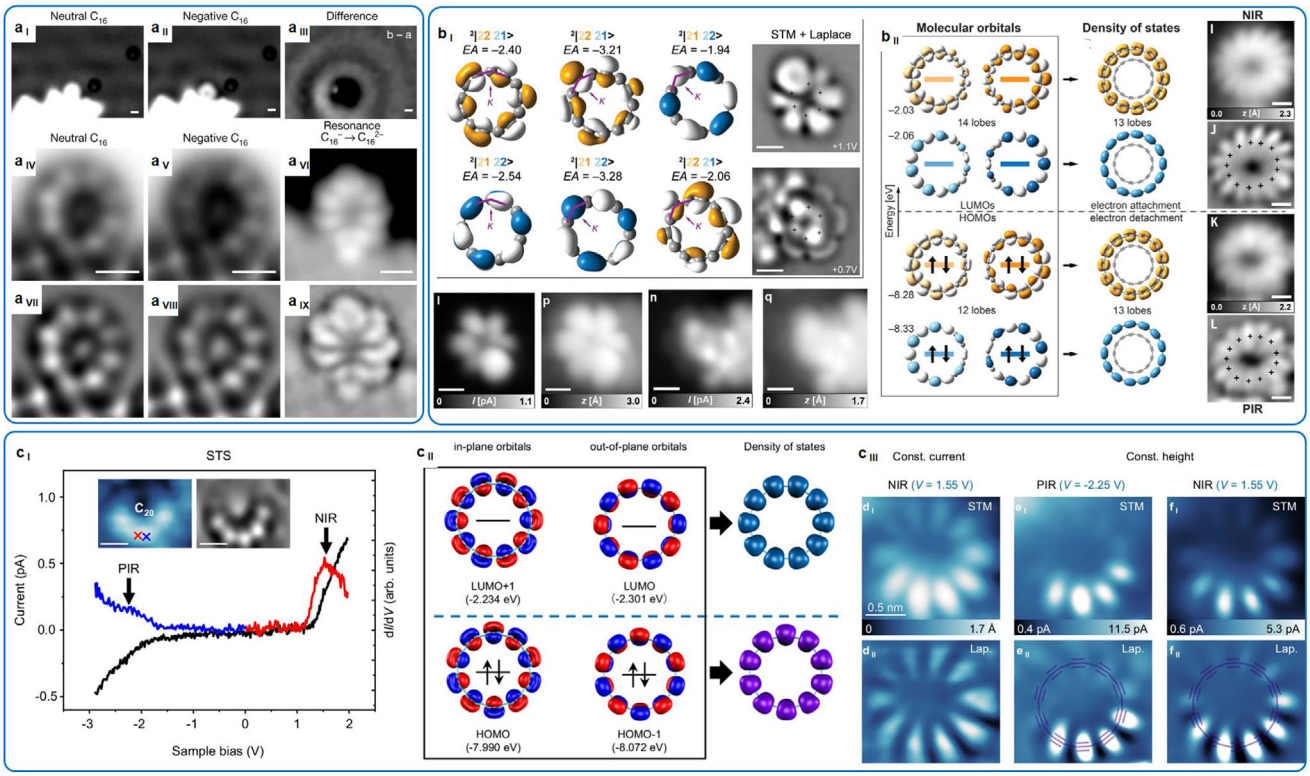

Figure 5. Electronic characterization of cyclo[*n*]carbons. a) Electronic characterization of C16. a $_{I}$-a $_{III}$) Constant-current STM images of C_{16} in neutral (a $_{I}$) and negative charge state (a $_{II}$), and difference of panels a_{II} and a_{I} (a_{III}). Constant-height AFM images of C_{16}^{0} (a $_{IV}$) and C_{16}^{-} (a $_{V}$). Constant-current STM (a $_{VI}$) mapping the ionic resonance of C_{16}^{-} to C_{16}^{2-}. a $_{VII}$-a $_{IX}$) Corresponding Laplace filter. Reproduced with permission.[58] Copyright 2023, The Author(s). b) Electronic characterization of C_{13} and C_{26}. b $_{I}$) Dyson orbitals for the two different anionic charge states. Laplace-filtered STM images of kinked C_{13} at indicated V, corresponding to out-of-plane and in-plane orbitals. b $_{II}$) Frontier molecular orbitals, superposition of orbital, densities of the respective energy degenerate orbital pairs, STM data at NIR and PIR and corresponding Laplace filtered images. Reproduced with permission. Reproduced with permission.[62] Copyright 2024, The Authors. c) Electronic characterization of cyclo[20]carbon. c $_{I}$) STS of C_{20} conducted on NaCl. c $_{II}$) Calculated frontier orbitals of C_{20} and superposition of orbital densities of the nearly energetically degenerated orbitals. c $_{III}$) STM images and Laplace-filtered STM images of C_{20} obtained with a CO-tip, including NIR, constant current mode; PIR, constant height mode and NIR, constant height mode. Reproduced with permission[65] Copyright 2024, The Author(s).

on ML NaCl. The shape of the molecule was influenced by the surface environment due to different adsorption sites. Interestingly, C_{26} can be generated through tip-induced molecular fusion of two precursors. The corresponding AFM image displays a ring structure with 13 triple bonds, indicating a polyynic structure.

3.2. Electronic Characterization of Cyclo[*n*]Carbons

Theoretical works have predicated lots of fascinating properties of cyclocarbons, for example, owing two delocalized π electron systems.[83] However, characterizations of their electronic structures are extremely difficult, as the small size of cyclocarbons and a high surface mobility. Recently, some attempts are conducted to characterize the electronic properties of cyclocarbons by blocking their diffusions on NaCl surfaces.

In literature, C_{18} is generally neutral and charged on NaCl surfaces, exhibiting charge bistability. Negatively charged C_{18} adopts a less symmetric and less planar geometry compared to neutral one, which is triggered by STM imaging at 0.6 V. The charged state is evidenced by the appearance of standing wave pattern in STM image. C_{16} also exhibits both neutral and charged states. When a bias of 0.5 V is applied, C_{16} transitions from a neutral state to a negatively charged state, and this transition reverses at a bias of −0.3 V. The C_{16} molecules are stabilized by adsorption on the edge of the third step. At 1.2 V, the orbital density corresponding to the electron resonance during the transition of C_{16}^{-} anions to C_{16}^{2-} anions is observed (**Figure** 5a$_{VI}$).

Smaller odd-numbered cyclocarbon, C_{13}, have also been studied by attaching them to the edges of NaCl to measure their electronic properties. At V = +0.8 V, STM images reveal the NIR of C_{13}, with bright spots located above each single bond. These bright spots correspond to the out-of-plane Dyson orbitals. The STM maps of C_{26} display characteristic features with 13 lobes (Figure 5b$_{II}$) at both NIR (V = 2.0 V) and PIR (V = −2.75 V). For NIR, the energy-degenerate LUMO superposition results in 14 lobes, with high-density lobes located above the long bonds. For PIR, the lobes are positioned above the triple bonds, and the energy density superposition leads to the formation of HOMO. The out-of-plane orbitals expose a greater orbital density under the tip, which dominates the STM contrast and is nearly degenerate with the in-plane orbitals. The out of plane HOMO (HOMO-2, and

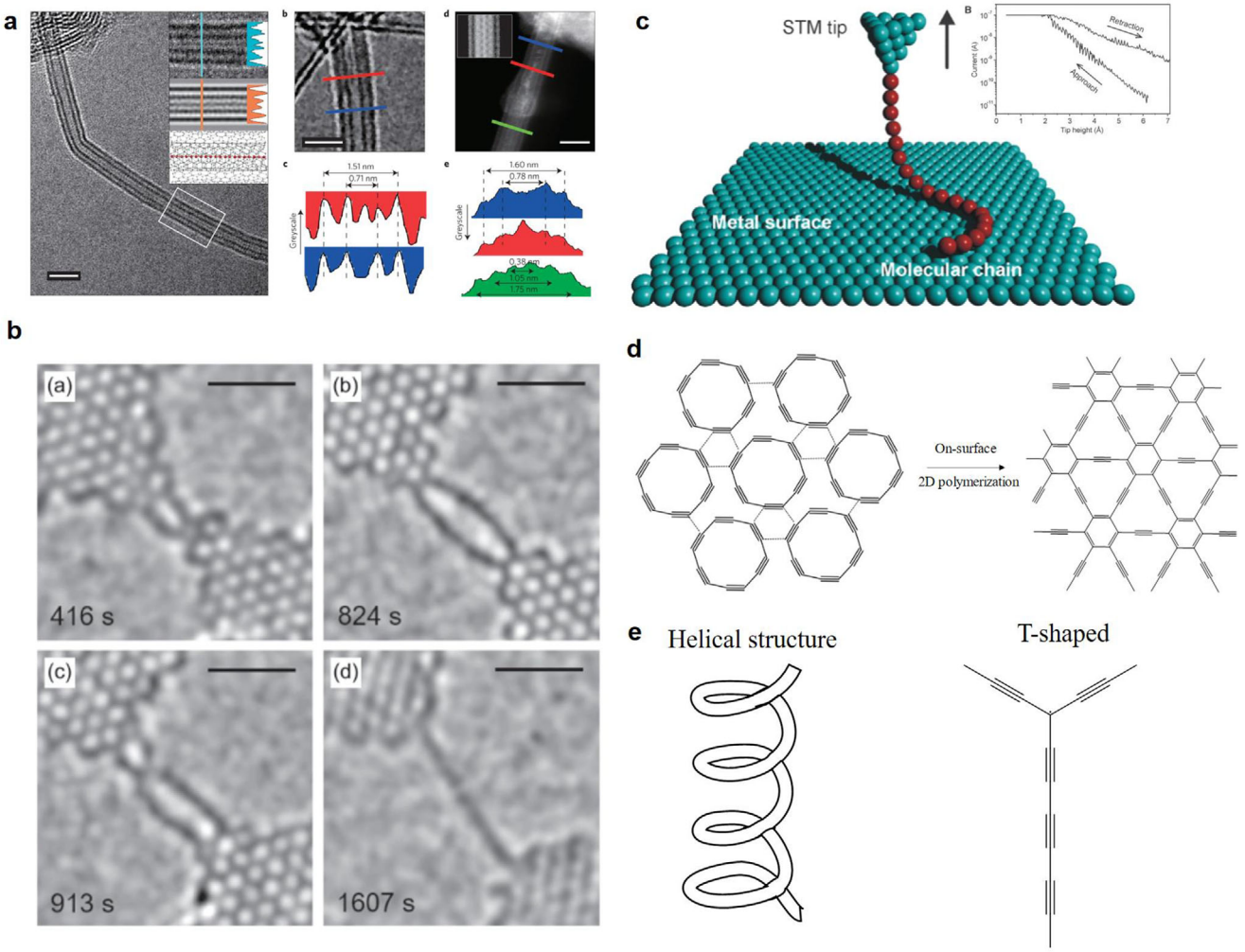

Figure 6. Outlook of sp-hybridized carbon allotropes. a) Direct observation of LCCs@DWCNTs. Reproduced with permission.[105] Copyright 2016, Springer Nature Limited. b) Aberration-corrected TEM images of an electron beam sculptured graphene nanoribbon. Images were recorded as carbon atoms were gradually removed by the electron beam, showing how the constriction reconstructs into a grafted cyclocarbon, then breaks to leave a single polyyne chain. Reproduced with permission.[106] Copyright 2014, American Chemical Society. c) Scheme of lifting a single molecular chain with the STM tip and tunneling current as a function of the tip height during a vertical manipulation Reproduced with permission.[107] Copyright 2009, The American Association for the Advancement of Science. d) Synthetic approach from C_{12} to the infinite network graphyne, proposed by Diederich.[108] e) Helical structure and T-shaped structure of carbon chains.

HOMO-3) each have 12 lobes, which superimpose to produce 13 lobes.

In addition to using NaCl edge, Cl atoms were also used to characterize the electronic properties of C_{20}. Subtly positioning the C_{20} molecule into an atomic fence formed by Cl clusters allows to experimentally probe its frontier molecular orbitals. As shown in Figure 5c$_{I}$, there are two peaks in the dI/dV of C_{20} at V = −2.25 V and V = 1.55 V, corresponding to PIR and NIR, respectively, yielding a transport gap of 3.8 eV. In PIR (Figure 5c$_{III}$), ten lobes are displayed over each triple bond, corresponding to the superposition state of nearly degenerated HOMO (in plane) and HOMO-1 (out of plane). In NIR (Figure 5c$_{III}$), ten bright lobes are located over each single bond, corresponding to the superposition of LUMO (out of plane) and LUMO+1 (in plane). The peaks of PIR and NIR are mainly related to out of plane orbitals, i.e., HOMO-1 and LUMO.

4. Conclusion and Perspective

In summary, we have comprehensively summarized the recent breakthroughs on the on-surface synthesis and characterization of sp-hybridized carbon allotropes, including linear carbon chains and cyclocarbons. On-surface synthesis enables the creation of high reactive species that are otherwise difficult to achieve through solution chemistry. Using on-surface synthesis, researchers have developed a set of sophisticated strategies, and generated sp-hybridized carbon allotropes with remarkable bond-resolved level. Scientists have used the tip-induced chemistry, achieving the synthesis of C_{18} and C_{16}. Combined with tip-induced dehalogenation and retro-Bergman ring-opening reaction, other cyclocarbons, e.g., C_{10}, C_{12}, C_{13}, C_{14}, C_{20}, C_{26} were generated on surface. Through the state-of-art characterization techniques, they have unraveled unique geometric and electronic

structures of these species. We expect that more exciting works in this area continue to appear in the future.

It has been demonstrated that removing metal atoms from metalated carbyne could be a feasible way to generating LCCs. While, a large area of generation of LCCs has not been achieved. Moreover, these LCCs are still terminated with other groups, for example, metalated carbyne. The generation of pure LCCs without terminated groups remains challenging.

In addition, other synthetic pathways could also be employed to generate and characterize LCCs. For example, **Figure 6a** shows DWCNTs protected the preparation of LCCs. Figure 6b shows a method of controllably manipulating the removal of carbon atoms from graphene using the transmission electron microscopy technique.[105] Figure 6c shows the measurements of the relationship between the electrical conductivity and the length of carbon chains through STM lifting technique.[107,109]

Carbon chains can form various structures, such as helical structures and T-shaped structures. Helical structures have special conductance characteristics.[110] When bent into a helix, it introduces integer multiples of narrow conductance drops related to the pitch and radius, and the conductance of a finite-length helical structure shows oscillatory behavior, with the frequency depending on the radius and pitch.[111] The T-shaped structure changes the double bond at the junction into a planar-like bonding, altering the local electronic structure. Constructing complex structures like T-shaped and cross-shaped ones can change the electron transmission path and charge distribution, thus regulating the overall electronic performance.[112]

The tip manipulation technique has been demonstrated to be a powerful and efficient method to generate cyclocarbons on surface. While, this methods are inadequate when it comes to large-scale fabrication, which remains a fertile ground that warrants extensive exploration.[113] To tackle this issue, we could broaden the utilization of tip manipulation technology in tandem with artificial intelligence (AI) manipulation strategies. For example, AI-powered automated molecular manipulation could be adopted to actualize automated production.[114–117] This might entail integrating specific methods for automatic scanning and the precise application of pulses.[114,115]In addition, using machine learning to analyze and glean insights from extensive historical experimental data could benefit the derive reference reaction conditions.[118] Through such means, it is very promising to surmount the existing limitations in the synthesis of cyclocarbons and edging closer to more streamlined, efficient, and productive manufacturing processes.

Carbynes have an effective surface area of $\approx 1300\ m^2\ kg^{-1}$, four times greater than graphene's theoretical value.[119] Their thermal conductivity ranges from 200 to 80 kW mK^{-1}, exceeding that of graphene and carbon nanotubes.[120] High-frequency phonons in the chains can travel long distances with minimal scattering, enabling thermal transport over micrometer scales. As the number of atoms in the chain increases, the optical absorption rate also rises, reaching up to 7.5×10^5 L mol^{-1} cm^{-1}.[67] The formation of atomic carbon chains has been proposed to explain the behavior of graphene-based molecular switches.[121]

Cyclocarbons, a captivating class of carbon allotropes, have garnered significant attention due to their unique electronic, mechanical, and optical properties. Recent computational studies have provided valuable insights into the characteristics of these molecules, particularly focusing on cyclo[18]carbon. C_{18} exhibits distinct aromaticity and an extensive π electron system delocalized across the entire ring, resulting in excellent electrical conductivity.[123] This, coupled with its ohmic and quasi-Schottky characteristics, suggests its potential for use in molecular electronics.[123] C_{18} is also predicted to be ultra elastic with a small Young's modulus and tensile stiffness, making it suitable for flexible and durable materials.[122] The bandgap of C_{18} is not fixed and can be altered by expanding the ring structure, offering possibilities for optical applications.[122] Devices based on C_{18} molecules have shown switching effects and negative differential resistance (NDR), which are highly desirable in nanoscale electronics. Incorporating C_{18} into molecular devices can provide current-limiting abilities, enhancing the performance and reliability of these devices. An innovative application involves using zigzag graphene nanoribbons (ZGNRs) with C_{18} to achieve dual spin filtering effects and realize NDR.[123] Inserting a metal carbon chain between nonmagnetic ZGNRs and C_{18} can lead to specific molecular configurations that further enhance the functionality of these hybrid structures, opening up new avenues for spintronics and advanced electronic devices.[124]

To employ the sp-hybridized carbon allotropes into a real device, the transfer to a more suitable substrate is still highly challenging. The carbon allotropes could disappear or polymerize during transfer. In addition, any contamination could affect the properties of devices. This direction is promising but very challenging in the application of these unique carbon allotropes. Diederich et al. hypothesized that cyclo[*n*]carbon could be used as a precursor for synthesizing graphdiyne.[108] Following a similar line of thought, the use of a C_{12} precursor might enable the synthesis of graphyne. Similar to linear carbon, cyclocarbons can also serve as a potential precursor for the formation of other carbon structures, which contributes to our understanding of the evolution of carbon allotropes.[125] Looking ahead, sp-hybridized carbon allotropes have broad application prospects in the field of materials science.0

Acknowledgements

Y.G. and W.X. contributed equally to this work. The authors acknowledge the financial support from the National Natural Science Foundation of China (22125203, 22402149), and the National Key R&D Program of China (2023YFE0101900), the Ministry of Science and Technology of the People's Republic of China, and the Shanghai Science and Technology Program (24ZR1470000).

Conflict of Interest

The authors declare no conflict of interest.

Keywords

carbon allotropes, carbyne, cyclo[*n*]carbon, on-surface synthesis, sp-hybridized

Received: January 19, 2025
Revised: April 5, 2025
Published online:

[1] T. Henning, F. Salama, *Science* **1998**, *282*, 2204.
[2] F. Ahmad, A. Mahmood, T. Muhmood, *Heteroatom-Doped Carbon Allotropes: Progress in Synthesis, Characterization, and Applications*, American Chemical Society, Washington, DC **2024**, Vol. *1491*, p. 349-350.
[3] A. Hirsch, *Nat. Mater.* **2010**, *9*, 868.
[4] H. R. Karfunkel, T. Dressler, A. Hirsch, *J. Comput.-Aided Mol. Des.* **1992**, *6*, 521.
[5] F. Diederich, *Nature* **1994**, *369*, 199.
[6] M. A. White, S. Kahwaji, V. L. S. Freitas, R. Siewert, J. A. Weatherby, M. D. M. C. Ribeiro da Silva, S. P. Verevkin, E. R. Johnson, J. W. Zwanziger, *Angew. Chem., Int. Ed.* **2021**, *60*, 1546.
[7] F. P. Bundy, W. A. Bassett, M. S. Weathers, R. J. Hemley, H. U. Mao, A. F. Goncharov, *Carbon* **1996**, *34*, 141.
[8] F. Lavini, M. Rejhon, E. Riedo, *Nat. Rev. Mater.* **2022**, *7*, 814.
[9] D. D. L. Chung, *J. Mater. Sci.* **2002**, *37*, 1475.
[10] J. Hu, J. Yu, Y. Li, X. Liao, X. Yan, L. Li, *Nanomaterials* **2020**, *10*, 664.
[11] Y. Xu, Z. Lin, X. Zhong, X. Huang, N. O. Weiss, Y. Huang, X. Duan, *Nat. Commun.* **2014**, *5*, 4554.
[12] H. W. Kroto, J. R. Heath, S. C. O'Brien, R. F. Curl, R. E. Smalley, *Nature* **1985**, *318*, 162.
[13] Y. Liu, S. C. O'Brien, Q. Zhang, J. R. Heath, F. K. Tittel, R. F. Curl, H. W. Kroto, R. E. Smalley, *Chem. Phys. Lett.* **1986**, *126*, 215.
[14] H. Kroto, *Angew. Chem., Int. Ed.* **1997**, *36*, 1578.
[15] L. T. Scott, M. M. Boorum, B. J. McMahon, S. Hagen, J. Mack, J. Blank, H. Wegner, A. de Meijere, *Science* **2002**, *295*, 1500.
[16] S. Iijima, *Nature* **1991**, *354*, 56.
[17] S. Rathinavel, K. Priyadharshini, D. Panda, *Mater. Sci. Eng. B-Adv. Funct. Solid-State Mater.* **2021**, *268*, 115095.
[18] R. Andrews, M. C. Weisenberger, *Curr. opin. Solid State Mat. Sci.* **2004**, *8*, 31.
[19] K. S. Novoselov, A. K. Geim, S. V. Morozov, D. Jiang, Y. Zhang, S. V. Dubonos, I. V. Grigorieva, A. A. Firsov, *Science* **2004**, *306*, 666.
[20] H. Murata, Y. Nakajima, N. Saitoh, N. Yoshizawa, T. Suemasu, K. Toko, *Sci. Rep.* **2019**, *9*, 4068.
[21] A. H. Castro Neto, F. Guinea, N. M. R. Peres, K. S. Novoselov, A. K. Geim, *Rev. Mod. Phys.* **2009**, *81*, 109.
[22] A. Joseph, V. Sajith, C. Sarathchandran, S. Thomas, C. Sarathchandran, S. A. Ilangovan, J. C. Moreno-Piraján, *Handbook of Carbon-Based Nanomaterials*, Elsevier, Amsterdam **2021**.
[23] X.-Y. Fang, X.-X. Yu, H.-M. Zheng, H.-B. Jin, L. Wang, M.-S. Cao, *Phys. Lett. A* **2015**, *379*, 2245.
[24] J. H. Gosling, O. Makarovsky, F. Wang, N. D. Cottam, M. T. Greenaway, A. Patanè, R. D. Wildman, C. J. Tuck, L. Turyanska, T. M. Fromhold, *Commun. Phys.* **2021**, *4*, 30.
[25] A. K. Geim, K. S. Novoselov, *Nat. Mater.* **2007**, *6*, 183.
[26] K. Luo, B. Liu, W. Hu, X. Dong, Y. Wang, Q. Huang, Y. Gao, L. Sun, Z. Zhao, Y. Wu, Y. Zhang, M. Ma, X. F. Zhou, J. He, D. Yu, Z. Liu, B. Xu, Y. Tian, *Nature* **2022**, *607*, 486.
[27] B. Li, B. Liu, K. Luo, K. Tong, Z. Zhao, Y. Tian, *Acc. Mater. Res.* **2024**, *5*, 614.
[28] Y. Ge, K. Luo, Y. Liu, G. Yang, P. Ying, Y. Wu, K. Tong, B. Liu, B. Li, G. Gao, X.-F. Zhou, Z. Zhao, B. Xu, Y. Tian, *Appl. Phys. Rev.* **2023**, *10*, 021418.
[29] B. Li, K. Luo, Y. Ge, Y. Zhang, K. Tong, B. Liu, G. Yang, Z. Zhao, B. Xu, Y. Tian, *Carbon* **2023**, *203*, 357.
[30] Y. Ge, K. Luo, Y. Liu, G. Yang, W. Hu, B. Li, G. Gao, X.-F. Zhou, B. Xu, Z. Zhao, Y. Tian, *Mater. Today Phys.* **2022**, *23*, 100630.
[31] Y. Wang, P. Yang, L. Zheng, X. Shi, H. Zheng, *Energy Storage Mater.* **2020**, *26*, 349.
[32] M. C. McCarthy, P. Thaddeus, *Chem. Soc. Rev.* **2001**, *30*, 177.
[33] L. N. Zack, J. P. Maier, *Chem. Soc. Rev.* **2014**, *43*, 4602.
[34] J. P. Maier, E. K. Campbell, *Angew. Chem., Int. Ed.* **2017**, *56*, 4920.
[35] M. Liu, V. I. Artyukhov, H. Lee, F. Xu, B. I. Yakobson, *ACS Nano* **2013**, *7*, 10075.
[36] D. C. Parent, S. W. McElvany, *J. Am. Chem. Soc.* **1989**, *111*, 2393.
[37] A. Van Orden, R. J. Saykally, *Chem. Rev.* **1998**, *98*, 2313.
[38] M. Grutter, M. Wyss, E. Riaplov, J. P. Maier, S. D. Peyerimhoff, M. Hanrath, *J. Chem. Phys.* **1999**, *111*, 7397.
[39] K. S. Pitzer, E. Clementi, *J. Am. Chem. Soc.* **1959**, *81*, 4477.
[40] V. Parasuk, J. Almlof, M. W. Feyereisen, *J. Am. Chem. Soc.* **1991**, *113*, 1049.
[41] S. W. McElvany, M. M. Ross, N. S. Goroff, F. Diederich, *Science* **1993**, *259*, 1594.
[42] R. J. Meilunas, R. P. H. Chang, *J. Mater. Res.* **1994**, *9*, 61.
[43] B. Pan, J. Xiao, J. Li, P. Liu, C. Wang, G. Yang, *Sci. Adv.* **2015**, *1*, 1500857.
[44] R. J. Lagow, J. J. Kampa, H.-C. Wei, S. L. Battle, J. W. Genge, D. A. Laude, C. J. Harper, R. Bau, R. C. Stevens, J. F. Haw, E. Munson, *Science* **1995**, *267*, 362.
[45] J. Cai, P. Ruffieux, R. Jaafar, M. Bieri, T. Braun, S. Blankenburg, M. Muoth, A. P. Seitsonen, M. Saleh, X. Feng, K. Mullen, R. Fasel, *Nature* **2010**, *466*, 470.
[46] D. J. Rizzo, G. Veber, T. Cao, C. Bronner, T. Chen, F. Zhao, H. Rodriguez, S. G. Louie, M. F. Crommie, F. R. Fischer, *Nature* **2018**, *560*, 204.
[47] N. Pavlicek, A. Mistry, Z. Majzik, N. Moll, G. Meyer, D. J. Fox, L. Gross, *Nat. Nanotechnol.* **2017**, *12*, 308.
[48] J. Su, M. Telychko, P. Hu, G. Macam, P. Mutombo, H. Zhang, Y. Bao, F. Cheng, Z.-Q. Huang, Z. Qiu, S. J. R. Tan, H. Lin, P. Jelínek, F.-C. Chuang, J. Wu, J. Lu, *Sci. Adv.* **2019**, *5*, aav7717.
[49] X. Li, H. Zhang, L. Chi, *Adv. Mater.* **2019**, *31*, 1804087.
[50] X. Li, Z. Xu, D. Bu, J. Cai, H. Chen, Q. Chen, T. Chen, F. Cheng, L. Chi, W. Dong, Z. Dong, S. Du, Q. Fan, X. Fan, Q. Fu, S. Gao, J. Guo, W. Guo, Y. He, S. Hou, Y. Jiang, H. Kong, B. Li, D. Li, J. Li, Q. Li, R. Li, S. Li, Y. Lin, M. Liu, *et al.*, *Chin. Chem. Lett.* **2024**, *35*, 110055.
[51] X. Li, Z. Xu, D. Bu, J. Cai, H. Chen, Q. Chen, T. Chen, F. Cheng, L. Chi, W. Dong, Z. Dong, S. Du, Q. Fan, X. Fan, Q. Fu, S. Gao, J. Guo, W. Guo, Y. He, S. Hou, Y. Jiang, H. Kong, B. Li, D. Li, J. Li, Q. Li, R. Li, S. Li, Y. Lin, M. Liu, *et al.*, *Chin. Chem. Lett.* **2025**, *36*, 110100.
[52] S. Fang, Y. H. Hu, *Matter* **2021**, *4*, 1189.
[53] F. J. Giessibl, *Rev. Sci. Instrum.* **2019**, *90*, 011101.
[54] S. Clair, D. G. de Oteyza, *Chem. Rev.* **2019**, *119*, 4717.
[55] L. Grill, S. Hecht, *Nat. Chem.* **2020**, *12*, 115.
[56] L. Grill, M. Dyer, L. Lafferentz, M. Persson, M. V. Peters, S. Hecht, *Nat. Nanotechnol.* **2007**, *2*, 687.
[57] Q. Fan, L. Yan, M. W. Tripp, O. Krejčí, S. Dimosthenous, S. R. Kachel, M. Chen, A. S. Foster, U. Koert, P. Liljeroth, J. M. Gottfried, *Science* **2021**, *372*, 852.
[58] Q. Zhong, A. Ihle, S. Ahles, H. A. Wegner, A. Schirmeisen, D. Ebeling, *Nat. Chem.* **2021**, *13*, 1133.
[59] N. Pavliček, L. Gross, *Nat. Rev. Chem.* **2017**, *1*, 5.
[60] S.-W. Hla, L. Bartels, G. Meyer, K.-H. Rieder, *Phys. Rev. Lett.* **2000**, *85*, 2777.
[61] K. Kaiser, L. M. Scriven, F. Schulz, P. Gawel, L. Gross, H. L. Anderson, *Science* **2019**, *365*, 1299.
[62] F. Albrecht, I. Roncevic, Y. Gao, F. Paschke, A. Baiardi, I. Tavernelli, S. Mishra, H. L. Anderson, L. Gross, *Science* **2024**, *384*, 677.
[63] L. Sun, W. Zheng, W. Gao, F. Kang, M. Zhao, W. Xu, *Nature* **2023**, *623*, 972.
[64] Y. Gao, F. Albrecht, I. Rončević, I. Ettedgui, P. Kumar, L. M. Scriven, K. E. Christensen, S. Mishra, L. Righetti, M. Rossmannek, I. Tavernelli, H. L. Anderson, L. Gross, *Nature* **2023**, *623*, 977.
[65] L. Sun, W. Zheng, F. Kang, W. Gao, T. Wang, G. Gao, W. Xu, *Nat. Commun.* **2024**, *15*, 7649.
[66] W. A. Chalifoux, R. R. Tykwinski, *Nat. Chem.* **2010**, *2*, 967.
[67] C. S. Casari, A. Milani, *MRS Commun.* **2018**, *8*, 207.

[68] M. M. Haley, *Nat. Chem.* **2010**, *2*, 912.
[69] H. Cao, L. Shi, *Chin. Chem. Lett.* **2024**, *36*, 110466.
[70] K. Zhang, Y. Zhang, L. Shi, *Chin. Chem. Lett.* **2020**, *31*, 1746.
[71] X. Liu, G. Zhang, Y.-W. Zhang, *J. Phys. Chem. C* **2015**, *119*, 24156.
[72] B. V. Lebedev, *Russ. Chem. Bull.* **2000**, *49*, 965.
[73] C. S. Casari, M. Tommasini, R. R. Tykwinski, A. Milani, *Nanoscale* **2016**, *8*, 4414.
[74] C. Cignarella, D. Campi, N. Marzari, *ACS Nano* **2024**, *18*, 16101.
[75] Q. Sun, L. Cai, S. Wang, R. Widmer, H. Ju, J. Zhu, L. Li, Y. He, P. Ruffieux, R. Fasel, W. Xu, *J. Am. Chem. Soc.* **2016**, *138*, 1106.
[76] X. Yu, X. Li, H. Lin, M. Liu, L. Cai, X. Qiu, D. Yang, X. Fan, X. Qiu, W. Xu, *J. Am. Chem. Soc.* **2020**, *142*, 8085.
[77] W. Gao, F. Kang, X. Qiu, Z. Yi, L. Shang, M. Liu, X. Qiu, Y. Luo, W. Xu, *ACS Nano* **2022**, *16*, 6578.
[78] W. Gao, L. Cai, F. Kang, L. Shang, M. Zhao, C. Zhang, W. Xu, *J. Am. Chem. Soc.* **2023**, *145*, 6203.
[79] A. F. Hebard, M. J. Rosseinsky, R. C. Haddon, D. W. Murphy, S. H. Glarum, T. T. M. Palstra, A. P. Ramirez, A. R. Kortan, *Nature* **1991**, *350*, 600.
[80] X. F. Wang, R. H. Liu, Z. Gui, Y. L. Xie, Y. J. Yan, J. J. Ying, X. G. Luo, X. H. Chen, *Nat. Commun.* **2011**, *2*, 507.
[81] W. Gao, W. Zheng, L. Sun, F. Kang, Z. Zhou, W. Xu, *Natl. Sci. Rev.* **2024**, *11*, nwae031.
[82] N. Pavlicek, P. Gawel, D. R. Kohn, Z. Majzik, Y. Xiong, G. Meyer, H. L. Anderson, L. Gross, *Nat. Chem.* **2018**, *10*, 853.
[83] H. L. Anderson, C. W. Patrick, L. M. Scriven, S. L. Woltering, *Bull. Chem. Soc. Jpn.* **2021**, *94*, 798.
[84] F. Banhart, *ChemTexts* **2019**, *6*, 3.
[85] J. F. Hartwig, *Nat. Chem.* **2011**, *3*, 99.
[86] T. Torelli, L. Mitas, *Phys. Rev. Lett.* **2000**, *85*, 1702.
[87] C. Neiss, E. Trushin, A. Görling, *ChemPhysChem* **2014**, *15*, 2497.
[88] B. G. A. Brito, G. Q. Hai, L. Cândido, *Phys. Rev. A* **2018**, *98*, 062508.
[89] S. L. Wang, C. M. L. Rittby, W. R. M. Graham, *J. Chem. Phys.* **1997**, *107*, 6032.
[90] K. Raghavachari, D. L. Strout, G. K. Odom, G. E. Scuseria, J. A. Pople, B. G. Johnson, P. M. W. Gill, *Chem. Phys. Lett.* **1993**, *214*, 357.
[91] J. Hutter, H. P. Luethi, F. Diederich, *J. Am. Chem. Soc.* **1994**, *116*, 750.
[92] Y. Rubin, C. B. Knobler, F. Diederich, *J. Am. Chem. Soc.* **1990**, *112*, 4966.
[93] L. M. Scriven, K. Kaiser, F. Schulz, A. J. Sterling, S. L. Woltering, P. Gawel, K. E. Christensen, H. L. Anderson, L. Gross, *J. Am. Chem. Soc.* **2020**, *142*, 12921.
[94] Q. L. Lu, Y. C. Ling, Q. Luo, *Chem. Phys. Lett.* **2021**, *787*, 139221.
[95] S. Y. Pooja, R. Pawar, *Chem. Rec.* **2024**, *24*, 202400055.
[96] X. Wang, Z. Liu, X. Yan, T. Lu, W. Xiong, *Chem.-Eur. J.* **2022**, *28*, 202103815.
[97] Y. C. Ling, Q. L. Lu, Q. Luo, *Eur. Phys. J. D* **2021**, *75*, 229.
[98] Y. Wu, Z. Liu, T. Lu, M. Orozco-Ic, J. Xu, X. Yan, J. Wang, X. Wang, *Inorg. Chem.* **2023**, *62*, 19986.
[99] S. Haseena, K. R. Maiyelvaganan, M. Prakash, M. K. Ravva, *J. Mol. Struct.* **2022**, *1271*, 134025.
[100] S. Y. Pooja, R. Pawar, *Chem. Rec.* **2024**, *24*, 202400055.
[101] Z. Liu, T. Lu, Q. Chen, *Carbon* **2020**, *165*, 461.
[102] S. Furukawa, M. Fujita, Y. Kanatomi, M. Minoura, M. Hatanaka, K. Morokuma, K. Ishimura, M. Saito, *Comm. Chem.* **2018**, *1*, 60.
[103] P. W. Fowler, N. Mizoguchi, D. E. Bean, R. W. A. Havenith, *Chem. Eur. J.* **2009**, *15*, 6964.
[104] B. Schuler, S. Fatayer, F. Mohn, N. Moll, N. Pavlicek, G. Meyer, D. Pena, L. Gross, *Nat. Chem.* **2016**, *8*, 220.
[105] L. Shi, P. Rohringer, K. Suenaga, Y. Niimi, J. Kotakoski, J. C. Meyer, H. Peterlik, M. Wanko, S. Cahangirov, A. Rubio, Z. J. Lapin, L. Novotny, P. Ayala, T. Pichler, *Nat. Mater.* **2016**, *15*, 634.
[106] Y. Rong, J. H. Warner, *ACS Nano* **2014**, *8*, 11907.
[107] L. Lafferentz, F. Ample, H. Yu, S. Hecht, C. Joachim, L. Grill, *Science* **2009**, *323*, 1193.
[108] F. Diederich, Y. Rubin, *Angew. Chem., Int. Ed.* **1992**, *31*, 1101.
[109] S. You, C. Yu, Y. Gao, X. Li, G. Peng, K. Niu, J. Xi, C. Xu, S. Du, X. Li, J. Yang, L. Chi, *Nat. Commun.* **2024**, *15*, 6475.
[110] Z. Zanolli, G. Onida, J. C. Charlier, *ACS Nano* **2010**, *4*, 5174.
[111] S. Tongay, R. T. Senger, S. Dag, S. Ciraci, *Phys. Rev. Lett.* **2004**, *93*, 136404.
[112] R. Hoffmann, *Angew. Chem., Int. Ed.* **2003**, *26*, 846.
[113] H. J. Gao, L. Gao, *Prog. Surf. Sci.* **2010**, *85*, 28.
[114] N. Wu, M. Aapro, J. S. Jestila, R. Drost, M. M. Garcia, T. Torres, F. Xiang, N. Cao, Z. He, G. Bottari, P. Liljeroth, A. S. Foster, *J. Am. Chem. Soc.* **2024**, *147*, 1240.
[115] P. Leinen, M. Esders, K. T. Schütt, C. Wagner, K.-R. Müller, F. S. Tautz, *Sci. Adv.* **2020**, *6*, abb6987.
[116] I. J. Chen, M. Aapro, A. Kipnis, A. Ilin, P. Liljeroth, A. S. Foster, *Nat. Commun.* **2022**, *13*, 7499.
[117] B. Ramsauer, G. J. Simpson, J. J. Cartus, A. Jeindl, V. García-López, J. M. Tour, L. Grill, O. T. Hofmann, *J. Phys. Chem. A* **2023**, *127*, 2041.
[118] Z. Zhu, S. Yuan, Q. Yang, H. Jiang, F. Zheng, J. Lu, Q. Sun, *J. Am. Chem. Soc.* **2024**, *146*, 29199.
[119] P. B. Sorokin, H. Lee, L. Y. Antipina, A. K. Singh, B. I. Yakobson, *Nano Lett.* **2011**, *11*, 2660.
[120] M. Wang, S. Lin, *Sci. Rep.* **2015**, *5*, 18122.
[121] R. Tomov, M. Aleksandrova, *Molecules* **2023**, *28*, 6409.
[122] S. Fang, Y. H. Hu, *Carbon* **2021**, *171*, 96.
[123] Y. Xu, W. Wu, *J. Appl. Phys.* **2020**, *128*, 194303.
[124] L. Hou, H. Hu, G. Yang, G. Ouyang, *Phys. Status Solidi RRL* **2021**, *15*, 2000582.
[125] R. B. Heimann, R. B. Heimann, S. E. Evsyukov, L. Kavan, *Carbyne and Carbynoid Structures*, Springer, Dordrecht **1999**.

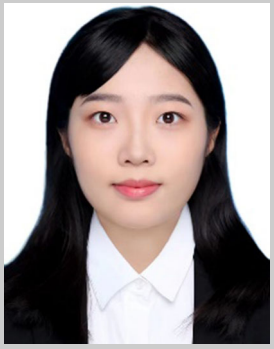

Yuan Guo received her bachelor's degree in engineering from Tongji University (School of Materials Science and Engineering), China in 2023. Since 2023, she has been working on the master's degree at the School of Materials Science and Engineering, Tongji University, under the supervision of Prof. Wei Xu. Her research interests include on-surface synthesis and characterization of molecular carbon allotropes using scanning probe microscopy.

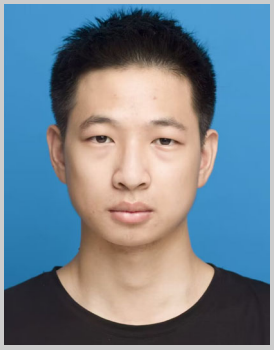

Wenzhi Xiang received his bachelor's degree in engineering from Hefei University of Technology (School of Materials Science and Engineering), China in 2023. Since 2023, he has been working on the master's degree at the School of Materials Science and Engineering, Tongji University, under the supervision of Prof. Xiaohui Qiu. His research interests include on-surface synthesis and characterization of molecular carbon allotropes using scanning probe microscopy.

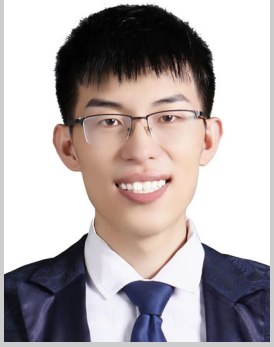

Luye Sun received his PhD degree from the National Center for Nanoscience and Technology, China in 2022 under the supervision of Prof. Xiaohui Qiu. Thereafter, he was engaged in the postdoctoral research at Tongji University (supervisor: Prof. Wei Xu). Since 2025, he started working in the School of Materials Science and Engineering at Tongji University, China, as an associate professor. His main research interests are on-surface synthesis and characterization of molecular carbon allotropes using scanning probe microscopy.

Wei Xu received his PhD degree in Science from Aarhus University, Denmark in 2008. Thereafter he was a postdoctoral fellow at Interdisciplinary Nanoscience Center (iNANO), Aarhus University, Denmark and at Departments of Chemistry and Physics, The Penn State University, USA. Since 2009 he has been a full professor at Tongji University, P. R. China. His main research interests are Scanning Tunneling Microscopy (STM) and Density Functional Theory (DFT) investigations of molecular self-assembly and reactions on surfaces under ultrahigh vacuum conditions with the aim of controllably building functional surface nanostructures and gaining fundamental insights into physics and chemistry.